ChemComm

Chemical Communications

www.rsc.org/chemcomm
Volume 49 | Number 53 | 7 July 2013 | Pages 5899–5998

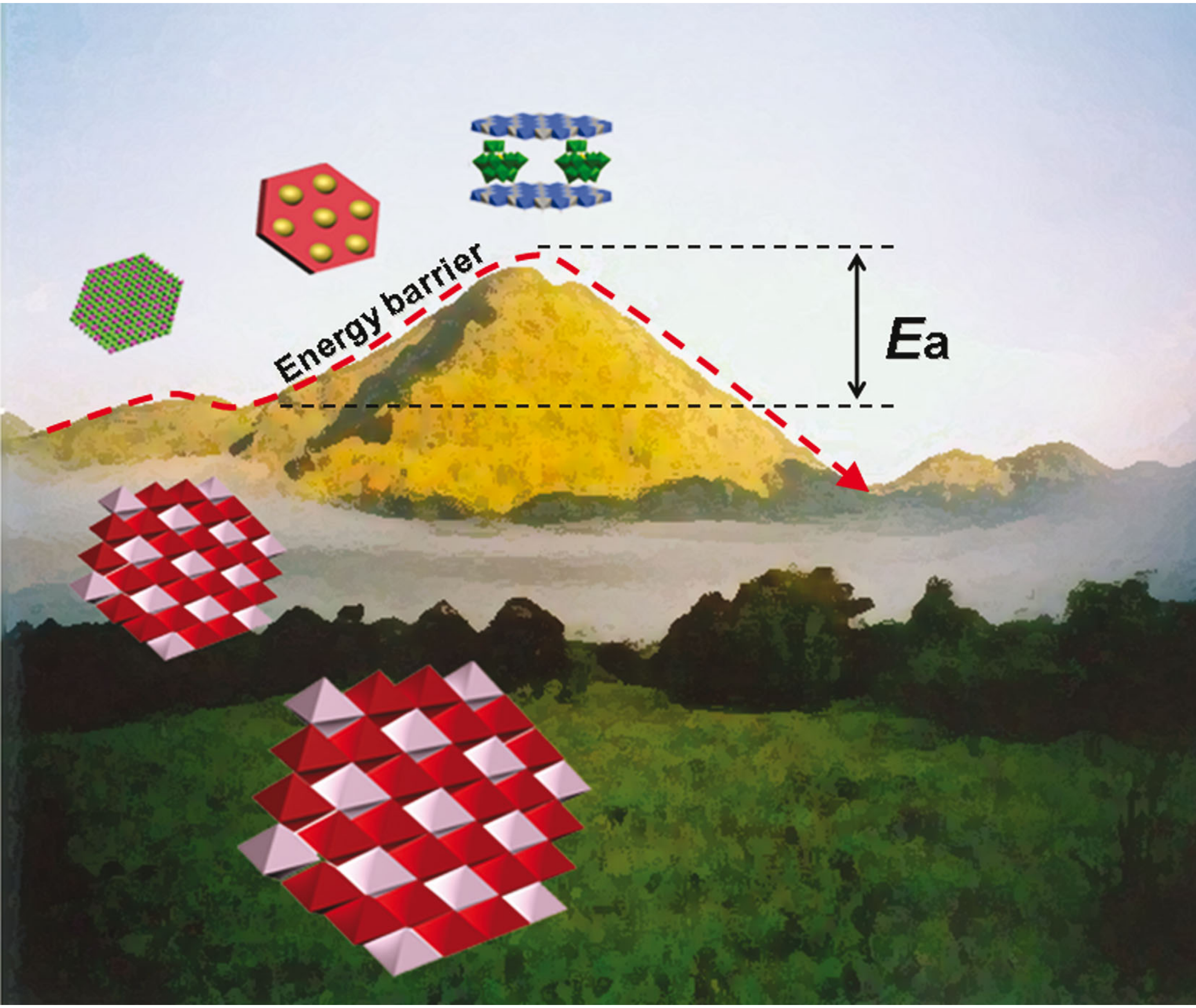

ISSN 1359-7345

RSC Publishing

FEATURE ARTICLE
Zhe An *et al.*
Layered double hydroxide-based catalysts: nanostructure design and catalytic performance

1359-7345(2013)49:53;1-Z

ChemComm

RSC Publishing

FEATURE ARTICLE

View Article Online
View Journal | View Issue

Layered double hydroxide-based catalysts: nanostructure design and catalytic performance

Cite this: *Chem. Commun.*, 2013, **49**, 5912

Shan He, Zhe An,* Min Wei, David G. Evans and Xue Duan

Received 24th March 2013,
Accepted 3rd May 2013

DOI: 10.1039/c3cc42137f

www.rsc.org/chemcomm

Published on 03 May 2013. Downloaded on 07/06/2013 03:35:59.

Layered double hydroxides (LDHs) are a class of clays with brucite-like layers and intercalated anions which have attracted increasing interest in the field of catalysis. Benefiting from the atomic-scale uniform distribution of metal cations in the brucite-like layers and the ability to intercalate a diverse range of interlayer anions, LDHs display great potential as precursors/supports to prepare catalysts, in that the catalytic sites can be preferentially orientated, highly dispersed, and firmly stabilized to afford excellent catalytic performance and recyclability. The approaches to prepare catalysts based on LDH materials include, but are not limited to, exfoliation of the brucite-like layers, lattice orientation/lattice confinement by the brucite-like layers, and intercalation. This *Feature Article* summarizes the latest developments in the design and preparation of nanocatalysts by using LDHs as precursors/supports.

1. Introduction

The design and preparation of heterogeneous catalysts with simultaneously enhanced activity and stability have attracted intense interest, in terms of both fundamental research and for their applications in the chemical industry. During the past thirty years, the formation of catalysts with effective control over small particle size and thus large specific surface areas, and their subsequent immobilization onto a suitable support have both been found to be effective ways of increasing catalyst activity and selectivity.[1–5] The catalytic properties of a material are determined by its electronic structure (especially the surface/interface electronic structure).[6–8] However, developing ways of tailoring the electronic structure of catalysts so as to enhance their heterogeneous catalytic performance is of vital importance and still remains a challenging goal. Many factors (*e.g.*, the surface morphology and the structure of active sites)—which are difficult to control using traditional methods of catalyst fabrication—have significant influences on the electronic structure of a catalyst. In recent years, nanotechnologies have been developed and widely applied in the controllable synthesis of various types of nanostructured catalysts with well-defined particle sizes, morphology, and compositions. Studies of the catalytic performance of these materials have further expanded our understanding of structure–property correlations.[9–13]

State Key Laboratory of Chemical Resource Engineering, Beijing University of Chemical Technology, Beijing 100029, China. E-mail: anzhe@mail.buct.edu.cn; Fax: +86-10-64425385; Tel: +86-10-64425280

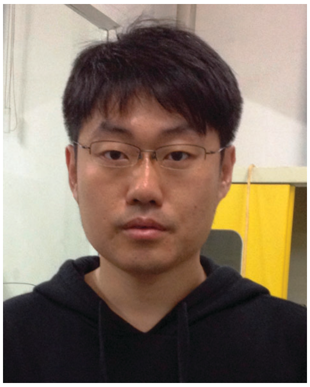

Shan He

Shan He received his BS degree in 2002 from Beijing Technology and Business University. He joined Professor Xue Duan's group as a PhD candidate at Beijing University of Chemical Technology in 2008, and he currently works on designing new catalysts based on layered double hydroxides.

Zhe An

Zhe An received her BSc (2005) and PhD (2011) degrees from Beijing University of Chemical Technology, where she mainly studied bio-inorganic hybrids based on layered double hydroxides, under the supervision of Prof. Jing He. After obtaining her PhD in 2011, she continued working at Beijing University of Chemical Technology. Her research interests focus on bio-inorganic hybrids, catalytic materials and environmentally friendly catalysis.

This journal is © The Royal Society of Chemistry 2013

Published on 03 May 2013. Downloaded on 07/06/2013 03:35:59.

Tailoring the electronic structure *via* tuning the nanostructure of catalysts so as to acquire the desired activity and selectivity is a promising approach.[14–17] Considerable interest has been focused on the design of the nanostructure of the catalytic active sites. Key issues include (i) how can the orientation of active sites be tuned to give the desired activity and selectivity? (ii) how can a high dispersion and adequate exposure of the active sites be realized in order to enhance the catalytic activity? (iii) how can the stability of active sites be improved so as to enhance the long-term catalytic stability? To date, the rational design and fabrication of nanoscale catalysts in order to satisfy these three requirements simultaneously remains a long-standing and fundamental scientific problem.

Layered double hydroxides (LDHs), also known as hydrotalcite-like materials, are a class of two-dimensional (2D) anionic clays consisting of positively charged host layers and exchangeable interlayer anions, which can be expressed by the formula $[M^{2+}_{1-x}M^{3+}_{x}(OH)_2](A^{n-})_{x/n}\cdot mH_2O$.[18–21] Recently, considerable attention has been focused on LDHs as sorbents and heterogeneous catalysts/precursors,[22–28] as a result of their versatility in chemical composition. A key structural characteristic of LDH materials is that the M^{II} and M^{III} cations are distributed in a uniform manner in the hydroxide layers,[29] without clusters of like cations. As a result they can be used as precursors or templates for the formation of nanocatalysts with specific morphology/surface structure and high dispersion. LDHs have also been proved to be effective supports for the immobilization of catalytically active anionic species in the interlayer region.[30] The uniform distribution of positive charges on the LDH layers facilitates the distribution and stability of the interlayer species through the electrostatic host–guest interactions. Moreover, LDH microcrystals can be exfoliated into positively-charged 2D nanosheets,[31] which can serve as building blocks for assembly with various catalytically active anions. Therefore, a variety of strategies—including exfoliation, lattice orientation/lattice confinement, and intercalation—are available for the fabrication of LDH-based nanocatalysts with preferential orientation, high dispersion and high stability of active sites.

An additional attractive feature of LDHs as far as catalysis is concerned, is that on calcination they are converted to high surface area mixed metal oxides (MMOs).[32–34] These materials are characterized by high surface area and are thus excellent supports for catalytically active species. Furthermore, if the LDH precursors contain transition metal ions these can be reduced *in situ* to give catalytically active metal particles supported on the remaining metal oxide phase.

In this *Feature Article*, we summarize recent progress in the design and preparation of highly efficient nanocatalysts based on LDHs and LDH-derived MMOs and highlight potential applications of these materials. In the final section, current challenges and future strategies are discussed from the viewpoint of catalyst design and catalytic performance. It is hoped that this *Feature Article* will focus more attention towards LDH-based nanocatalysts and encourage future work in this exciting area.

Min Wei

Min Wei obtained her BEng degree in 1995 and MEng degree in 1998 from Beijing University of Chemical Technology (BUCT). She subsequently received her PhD from Peking University in 2001, after which she joined the staff of BUCT. She was promoted to full professor in 2005. She was a visiting scholar at the Georgia Institute of Technology in 2008. Her research interests focus on inorganic–organic composite functional materials as well as new catalysts.

David G. Evans

David G. Evans studied as both an undergraduate and a research student at Jesus College, Oxford and obtained a DPhil under the supervision of Prof. D. M. P. Mingos FRS. After postdoctoral work at Bristol University with Prof. F. G. A. Stone FRS, he was appointed as a lecturer at Exeter University in 1985. Several visits to Chinese university chemistry departments in the early 1990s convinced him of China's great potential for development and he moved to Beijing University of Chemical Technology in 1996. His research interests focus on intercalation in layered solids. He was awarded an International Scientific and Technological Cooperation Award of the People's Republic of China in 2005.

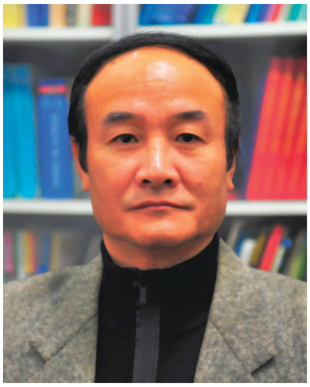

Xue Duan

Xue Duan was elected as an Academician of the Chinese Academy of Sciences in 2007 and a Fellow of the Royal Society of Chemistry in 2009. He was awarded his BS degree from Jilin University in 1982 and his PhD degree from the Chinese Academy of Sciences in 1988. He was subsequently appointed to the staff of Beijing University of Chemical Technology (BUCT) and established the Applied Chemistry Research Institute in 1990. He was promoted to full professor in 1993. He is currently a Director of the Institute of Applied Chemistry and an Executive Vice-Chair of the Academic Committee of the State Key Laboratory of Chemical Resource Engineering.

View Article Online

Published on 03 May 2013. Downloaded on 07/06/2013 03:35:59.

2. Nanocatalysts based on exfoliated LDH nanosheets

Recently, Wang and O'Hare *et al.*[35] have reviewed the various synthesis methods used to obtain positively charged dispersions of LDH nanosheets. By taking advantage of the electrostatic forces or/and hydrogen bonding between oppositely charged particles, nanocatalysts can be fabricated in a simple manner either *via* layer-by-layer (LBL) assembly of the LDH nanosheets with catalytically active anions, or alternatively these anions can be immobilized on the exfoliated LDH nanosheets themselves.[36,37] An example of the latter approach, involving the immobilization of amino acids for use as chiral ligands in the vanadium(V)-catalyzed asymmetric epoxidation of allylic alcohols with *tert*-butyl hydroperoxide (Bu^tOOH), is shown in Fig. 1. He *et al.*[38–40] compared the catalytic performance of a vanadium(V) precursor coordinated to the same amino acid ligands (a) in solution (a homogeneous catalyst), (b) after intercalation in a Zn/Al-LDH host (a heterogeneous catalyst), and (c) after immobilization on LDH nanosheets (a pseudo-homogeneous catalyst) produced by delamination of the amino acid anion-intercalated LDHs in formamide or water.

It was found that intercalating the amino acid ligands in the LDH sheets in (b) led to a significant increase in the enantiomeric selectivity of the catalysts compared with the homogeneous catalyst (a). This can be attributed to the access of reactant molecules to the active sites being restricted and/or directed by the large rigid inorganic layers. However the rate of reaction was slower for the heterogeneous catalyst. Delamination of the nanosheets in (c) allows the catalytic reactions to be carried out under pseudo-homogeneous reaction conditions, thereby significantly increasing the reaction rate while preserving the enhancement of the enantioselectivity afforded by anchoring the ligands on the LDH layers. Moreover, if the delamination is carried out in water, the colloidal catalyst can be directly separated from the products by simple liquid/liquid separation. The catalysts can be therefore easily recycled and show no loss of catalytic activity and enantioselectivity when reused.

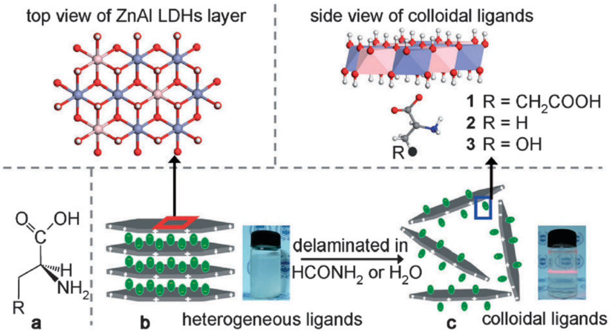

Fig. 1 Intercalation of the α-amino acids (1) L-glutamic acid, (2) L-alanine, and (3) L-serine (a) in an LDH host gives a heterogeneous catalyst precursor (b), whilst immobilization on delaminated LDH nanosheets gives a pseudo-homogeneous catalyst precursor (c). (● Zn ● Al ● N ● C ● O ● H; ◆ Zn–O octahedron ◆ Al–O octahedron). The materials obtained by treating (a)–(c) with VO(OPri3) were used as catalysts for the asymmetric epoxidation of allylic alcohols with Bu^tOOH. Reproduced with permission from ref. 38.

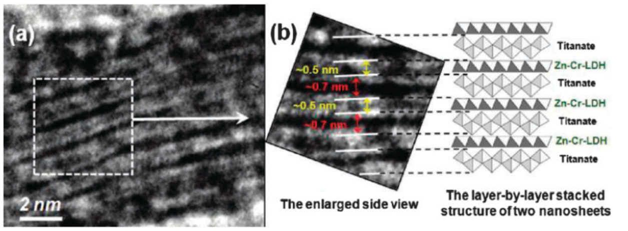

Fig. 2 (a) Cross-sectional high resolution transmission electron microscope (HRTEM) image of the mesoporous Zn/Cr-LDH nanosheet/layered titanate photocatalyst and (b) an enlarged view and structural model. Reproduced with permission from ref. 41.

An example of the alternative approach, whereby the exfoliated LDH nanosheets and the active species are combined *via* LBL assembly was recently reported by Gunjakar *et al.*,[41] who prepared mesoporous heterolayered photocatalysts by LBL assembly of Zn/Cr-LDH nanosheets and layered titanate nanosheets (Fig. 2), and showed that these possess a highly porous structure and visible-light harvesting ability due to the effective electronic coupling between cationic and anionic inorganic nanosheets. The resultant photocatalysts are fairly active for visible-light-induced O_2 generation with a rate of $\sim$1.18 mmol h^{-1} g^{-1}, which is higher than the rate of O_2 production ($\sim$0.67 mmol h^{-1} g^{-1}) with the pristine Zn/Cr-LDH material. Ordering of heterolayered photocatalysts is fairly important in optimizing visible-light-induced photocatalytic activity, and the chemical stability of the heterolayered photocatalysts is also significantly improved owing to the ordered structure of LDH nanosheets/layered titanate composite.

The positively-charged LDH nanosheets can also be used as building blocks for the fabrication of functional films by LBL assembly with oppositely charged electrocatalytically active species.[42,43] Wei *et al.*[44] have successfully fabricated LBL multilayers of Au nanoparticles (AuNPs) and LDH nanosheets on fluorine-doped tin oxide (FTO) substrates. Structural and morphological studies indicated that the $(LDH/AuNPs)_n$ ultrathin films (UTFs) exhibit long range stacking order, in which the AuNPs are highly dispersed and immobilized with a monolayer arrangement in the LDH gallery. This leads to the formation of electron tunneling junctions which facilitate electron transfer within the UTFs. The resulting $(LDH/AuNPs)_n$ UTFs display excellent electron transfer kinetics and electrocatalytic activity towards the oxidation of glucose (with a linear response range of 50 μM–20 mM and sensitivity of 343 μA mM^{-1} cm^{-2}) which is much higher than the corresponding values for previously reported AuNPs-based glucose sensors. Moreover, the $(LDH/AuNPs)_n$ UTFs also display very good long-term electrocatalytic stability.

3. Nanocatalysts based on orientation/confinement effects of LDHs

Metal catalysts supported on metal oxides prepared by conventional impregnation techniques often suffer from rapid deactivation (especially at high temperature) due to sintering/aggregation of the metal nanoparticles in a reaction system. A key structural

Published on 03 May 2013. Downloaded on 07/06/2013 03:35:59.

characteristic of LDH materials is that the M^{II} and M^{III} cations are distributed uniformly within the hydroxide layers.[29] If LDHs are converted to metal oxide-supported nanometal catalysts by heating under reducing conditions, the enhanced interactions between metal nanoparticles and the metal oxide substrate—which are formed concomitantly *in situ*—can prevent sintering/aggregation of the nanocatalyst during use and thus improves the stability of the active species. In addition, the topotactic nature of the LDH decomposition to metal oxide and/or the effect of confinement of a precursor in the LDH interlayer galleries can induce the formation of nanocatalysts with specific morphology, surface structure and high dispersion.[45,46]

3.1 Nanocatalysts with active species derived from LDH layers

Wei *et al.*[47,48] reported that well dispersed and embedded metallic iron nanoparticles with a high density (10^{14} to 10^{16} m^{-2}) and good thermal stability (at 900 °C) were obtained using MoO_4^{2-}-intercalated Fe/Mg/Al-LDHs as a precursor. The preparation of the metal nanoparticles is illustrated in Fig. 3. The MoO_4^{2-} anions were intercalated in the Fe/Mg/Al-LDHs by the calcinations–re-construction route. The MoO_4^{2-}–Fe/Mg/Al-LDHs were reduced to form well-dispersed Fe nanoparticles with high stability and control over size (3 to 20 nm) by means of a pinning effect of Mo around the Fe nanoparticles. These catalysts have a high density of metal nanoparticles and were active for the formation of single-walled carbon nanotube (SWNT)-array double helices. By virtue of the wide versatility of LDH composition and architecture, other metal nanoparticles with high dispersion, high density, and good thermal stability for catalysis can be fabricated *via* reduction of LDH precursors.[49–51] Recently, Zhang *et al.*[52] reported that a supported Ni catalyst with a high loading and good dispersion, prepared by using Ni/Al LDHs as a precursor, exhibited 100% conversion and 93% H_2 selectivity for the decomposition of hydrazine hydrate ($N_2H_4 \cdot H_2O$) at room temperature (as shown in Fig. 4). The activity and selectivity of this catalyst were much higher than those of a traditional supported Ni/Al_2O_3 catalyst (78 wt% Ni/Al_2O_3-IMP) with the same Ni loading prepared by the impregnation method (Fig. 4c). They proposed that the high H_2 selectivity of the LDH-derived catalyst originates from the cooperative effect of the small Ni particle size and strong basic sites located nearby. Furthermore the LDH-derived catalyst also showed excellent stability and when separated from the reaction medium—by taking advantage of the magnetic properties of the Ni particles—and reused, showed no significant loss in activity (Fig. 4d).

Bimetallic catalysts with rational design of the catalyst structure, giving enhanced stability, activity and selectivity have also been achieved by reduction of LDH precursors. Tomishige *et al.*[53] reported that uniform Ni–Fe alloy nanoparticles supported on Mg/Al MMOs with high dispersion were obtained by calcination and reduction of a Ni/Fe/Mg/Al-LDH precursor. In the steam reforming of toluene, the Ni–Fe/Mg–Al-MMO catalysts showed higher catalytic activity (a turnover frequency (TOF) of 1.3 s^{-1}) than Ni/Mg–Al-MMO (TOF: 0.8 s^{-1}), Ni/α-Al_2O_3 (TOF: 0.4 s^{-1}), and Ni–Fe/α-Al_2O_3. In addition, for longer reaction durations, Ni–Fe/Mg–Al-MMO maintained a toluene conversion of more than 99% for 20 h, indicating its high stability. This was attributed to aggregation of the nanoparticles being suppressed by their strong interaction with the MMO support. As other examples of intermetallic catalysts, Behrens *et al.*[54] have reported that well-dispersed and supported Pd_2Ga and PdZn particles could be synthesized by the reductive decomposition of ternary LDH compounds. The intermetallic catalysts were found to possess higher catalytic performance than a mono-metallic Pd catalyst in both methanol steam reforming and methanol synthesis from CO_2.

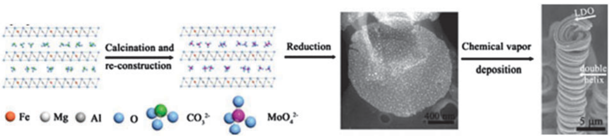

Fig. 3 Schematic illustration of the formation of high density metal nanoparticles from a precursor with MoO_4^{2-} incorporated in Fe/Mg/Al-LDHs. Reproduced with permission from ref. 47.

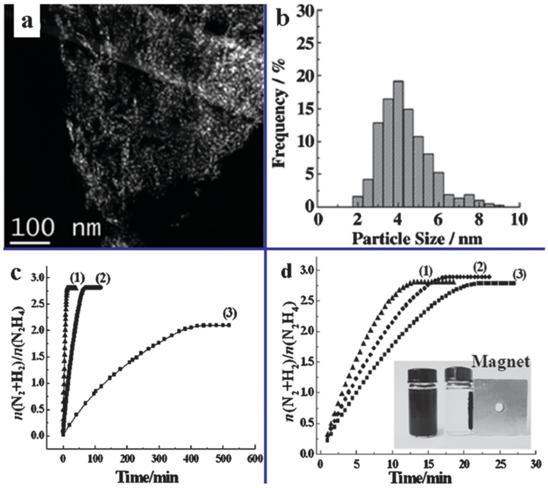

Fig. 4 (a) High angle annular dark field (HAADF) scanning transmission electron microscopy image of a Ni/Al_2O_3 catalyst produced by calcination and reduction of an LDH precursor at 500 °C; (b) histogram of the Ni particle size distribution; (c) plots of molar ratio $n(N_2 + H_2)/n(N_2H_4)$ *versus* time for the Ni/Al_2O_3-LDH-derived catalyst and 78 wt% Ni/Al_2O_3-IMP at different reaction temperatures: (1) Ni/Al_2O_3-LDH at 50 °C; (2) Ni/Al_2O_3-LDH at 308 °C; (3) 78 wt% Ni/Al_2O_3-IMP at 30 °C; (d) plots of $n(N_2 + H_2)/n(N_2H_4)$ *versus* time for Ni/Al_2O_3-LDH at 50 °C: (1) the second time; (2) the fifth time; (3) the tenth time. Inset: magnetic separation of the catalyst after reaction. Reproduced with permission from ref. 52.

For semiconductor nanoparticles with high photocatalytic efficiency, two features are believed to be essential—a high exposure of active facets and a high degree of dispersion. Wei *et al.*[55] reported ZnO nanoplatelets with a high degree of exposure of (0001) facets embedded on a hierarchical flower-like matrix, which were obtained *via* the *in situ* topotactic transformation process of a Zn/Al-LDH precursor. During the structural evolution of the Zn/Al-LDH precursor into the final ZnO-based MMO, a topotactic transformation based on the hexagonal structure of LDH is believed to occur, resulting in the formation of hexagonal ZnO nanoplatelets embedded on the ZnO-based MMO surface. As a result, hexagonal crystals of Zn/Al-LDH nanoflakes serve as both a ZnO source and a rigid template, which restrains the fast growth rate of ZnO along the

View Article Online

Published on 03 May 2013. Downloaded on 07/06/2013 03:35:59.

c-axis and induces the preferred growth of the nanoplatelets along the $[10\bar{1}0]$ direction. The resulting ZnO-based nanostructure exhibits both a high degree of preferred orientation and high dispersion, which displays superior visible-light photocatalytic activity to that of ZnO nanorods, ZnO nanoplates and the MMO powder sample. The high visible-light photocatalytic behaviour of this catalyst is possibly related to the presence of defects and edge dislocation in the exposed (0001) facets. In addition, the material maintains a constant photocatalytic activity over a number of consecutive cycles without peeling or aggregation of ZnO nanoplatelets.

3.2 Nanocatalysts supported on LDH layers or MMOs

LDH nanoflakes or MMOs can also serve as supports which can induce or/and restrict the formation of metal nanocatalysts with specific morphology and high dispersion by means of an exterior confinement effect from the LDH layers or MMO surface. Such an exterior confinement effect is effective in preventing the sintering/aggregation of nanoparticles, thus affording nanocatalysts with high stability.

Noble metal nanocrystals possess surface-dependent catalysis, which mainly originates from the different adsorption behavior of reactant molecules on various facets. The preferred formation/exposure of a specific facet of nanocrystals is a key factor contributing to enhanced activity and selectivity of catalysts. Li and Feng *et al.*[56,57] developed a new precipitation–reduction method to synthesize LDH-supported Pd catalysts with either tetrahedral or octahedral morphology (Fig. 5). In the synthesis process, hexamethylenetetramine was used not only to precipitate the LDH by virtue of the increase in pH associated with its hydrolysis, but also to reduce Pd^{2+} to Pd^0 nanoparticles, thus giving Pd/MgAl-CO_3-LDH in a single step. The resulting Pd nanoparticles were highly dispersed on the surface of the LDH platelets. In the selective hydrogenation of acetylene, tetrahedral particles with only Pd(111) facets exposed exhibited higher selectivity towards ethylene than truncated octahedral Pd particles enclosed by both Pd(111) and Pd(100) facets. Therefore, the Pd(111) facet can be regarded as the preferred facet in the selective hydrogenation of acetylene. In another example of the use of LDHs as a support for Pd catalysts, Choudary *et al.*[58] reported that nanopalladium particles supported on LDHs by a simple ion-exchange technique followed by reduction showed excellent yields and high TOF values in Heck-, Suzuki-, Sonogashira-, and Stille-type coupling reactions of chloroarenes, even deactivated chloroarenes. It was suggested that the basic LDH surface increases the electron density of the Pd center and promotes the oxidative addition of the normally unreactive chloroarene species. Furthermore, the catalyst can be quantitatively recovered unchanged from the reaction by a simple filtration and reused for a number of cycles with almost consistent activity in all the coupling reactions.

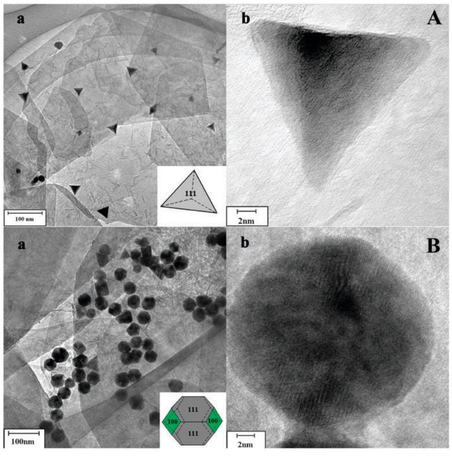

Fig. 5 HRTEM images of (A) tetra-Pd/MgAl-CO_3-LDH and (B) octa-Pd/MgAl-CO_3-LDH. Reproduced with permission from ref. 56.

Both LDH platelets themselves and the MMOs formed by their calcination have proved to be effective supports for nanogold catalysts. Zhang *et al.*[59] demonstrated the preferential deposition of gold nanoparticles (AuNPs) with a narrow size distribution (2–3 nm) on the lateral $(10\bar{1}0)$ facets of LDH platelets. The crystal face features of LDH platelets impose a crucial effect on the location and particle size of AuNPs. The lateral $(10\bar{1}0)$ facet with its high density of dangling bonds may have relatively active chemical characteristics, resulting in the preferential deposition of AuNPs on the $(10\bar{1}0)$ facet. Moreover, the strong interaction between the lateral $(10\bar{1}0)$ crystal facet and the AuNPs can prevent the aggregation of the latter particles. The crystal-face-selective supported AuNPs on the LDH can efficiently catalyze the epoxidation of styrene with Bu^tOOH as the oxidant; the TOF for styrene oxide production was 970 h^{-1}. Moreover, Kim *et al.*[60] reported that Au NPs-MMO nanocomposite photocatalysts can be prepared by an electrostatically driven self-assembly of dihydrolipoic acid-capped Au NPs and ZnAl-MMO nanoplates, which possess a negative and positive zeta potential, respectively. The Au NPs can be highly-dispersed on the ZnAl-MMO nanoplates with controlled morphology. The self-assembled nanocomposites exhibited superior self-sensitized dye degradation efficiency and photocatalytic stability under visible light compared with ZnO, TiO_2 (P25), or pure MMO nanoplates.

The synergistic effect between a metal nanocatalyst and an LDH support can effectively promote further enhancement of catalytic activity. Li, Hensen and co-workers.[61] have developed a novel and practical application of gold nanoparticles supported on a range of transition metal-containing LDHs as catalysts for the liquid-phase aerobic oxidation of alcohols in the absence of base additives. It was found that Au/MgCr-LDH gave a significantly higher benzaldehyde yield (76%) and TOF (1880 h^{-1}) than other transition metal containing LDH-based catalysts. The high activity of MgCr-LDH as a support was attributed to the fact that it not only offers surface basic sites like other LDH supports, but also surface chromium sites which participate in alcohol dehydrogenation. Moreover, in tests of the recycled catalyst, Au/MgCr-LDH showed a stable catalytic performance, and the average size and distribution of the Au nanoparticles was unchanged after reaction.

4. Nanocatalysts based on intercalation of catalytic active species

By taking advantage of the wide flexibility in the compensating anions which can be intercalated in their interlater galleries,

This journal is © The Royal Society of Chemistry 2013

Published on 03 May 2013. Downloaded on 07/06/2013 03:35:59.

LDHs containing a variety of catalytically-active species—including simple inorganic anions, complex anions and biomolecules—have been reported. In the last decade, it has been demonstrated that the intercalation of catalytically-active anions in LDHs is capable of improving their catalytic activity, selectivity and stability, compared with the homogeneous counterparts. LDHs offer a number of advantages as hosts for catalytically active anions: the electrostatic interactions between LDH layers and catalytically-active anions can induce an ordered arrangement of the anions and effectively tailor the orientation of the active site; the extent of the dispersion of the active sites can be controlled by modulation of the layer charge density (which depends on the ratio of M^{II} to M^{III} cations); the electrostatic interactions between LDH layers and catalytically-active anions can also lead to an increase in the stability of the latter.

Chiral amino acids and their derivatives have been widely employed as homogeneous catalysts for enantioselective processes, such as asymmetric aldol reactions and asymmetric amination.[62] Due to the drawbacks of homogeneous catalysts (short lifetime, low thermal stability, and difficulties in catalyst separation and recovery and product purification), much effort[63–69] has been dedicated to the immobilization of L-amino acids in LDHs. Wei *et al.*[70–72] reported the intercalation of L-tyrosine, L-aspartic acid and L-cysteine into the galleries of LDHs. It was found that the confinement effect of the host galleries effectively inhibited the racemization of guest L-amino acid anions under UV irradiation and thermal treatment. An *et al.*[73] synthesized a heterogeneous L-proline intercalated Mg/Al-LDH, which showed high enantiomeric excess (ee values of up to 94%) when used as a catalyst in aldol reactions, even under forcing conditions. The L-proline anions were shown to adopt an approximately horizontal orientation with respect to the hydroxide layers, with the carboxylate groups attaching directly to the hydroxide layers, and this enhanced the resistance of the catalyst to racemization at high temperatures or under UV irradiation (Fig. 6). Moreover, Vijaikumar *et al.*[74] showed that in the asymmetric Michael addition reaction between β-nitrostyrene and acetone, the LDH layers do not merely act as a support for L-proline anions but are also a cocatalyst for the reaction.

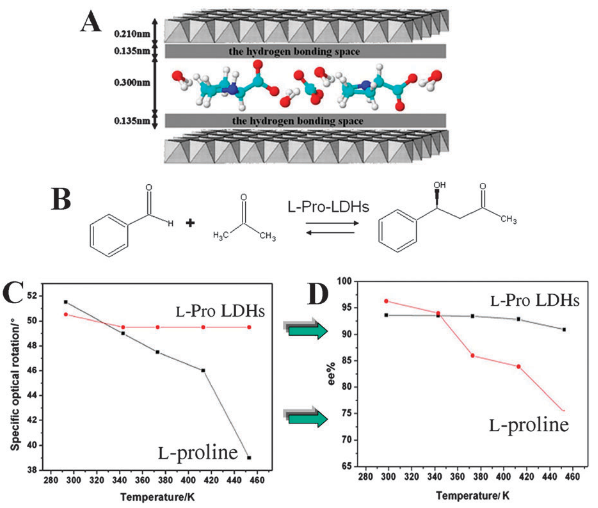

Fig. 6 (A) A schematic model of L-proline intercalated LDHs; Both (C) the thermal stability of specific optical rotation and (D) the enantiomeric excess (ee) value for the products of aldol reactions (B) are significantly improved after the L-proline catalyst is intercalated in an LDH host. Reproduced with permission from ref. 73.

The interlayer galleries of LDHs are also capable of accommodating much more bulky anions. The intercalation of large functional anions has been reported to afford enhanced catalytic activity in a number of catalytic processes, including the generation of singlet molecular oxygen from H_2O_2 over MoO_4^{2-} intercalated Mg/Al LDHs[75,76] or metal porphyrin complex intercalated LDHs,[77,78] *N*-oxidation of tertiary amines over WO_4^{2-} intercalated Mg/Al-LDHs,[79] epoxidation by salen–Mn(III) (salen = *N*,*N*′-ethylenebis(salicylimine)) intercalated Zn/Al-LDHs[80] or metal porphyrin intercalated LDHs,[81,82] and epoxidation reactions over polyoxometallate (POM) intercalated LDHs.[83,84] For example, Parida *et al.*[85] developed a novel heterogeneous catalyst by immobilizing a Ti(IV)-Schiff base complex in Zn/Al-LDH by an ion-exchange method. The performance of the immobilized catalyst in the epoxidation of cyclohexane (95% conversion of cyclohexene with 84% selectivity to cyclohexene oxide) carried out under solvent-free conditions was significantly better than the homogeneous counterpart (62% and 74%, respectively). The stability of the immobilized catalyst was also convincingly demonstrated by conducting three successive runs without appreciable loss of reactivity. Cu(II)[86] complexes of arylhydrazones of β-diketones (AHBDs) and La(III)[87] hydroxy citrate complexes intercalated in LDHs have been shown to catalyze the peroxidative oxidation of alkanes and the trans-esterification reaction of 1-phenylethanol with diethylcarbonate, showing enhanced catalytic activity compared with the homogeneous counterparts and good recyclability. Song *et al.*[88] reported $Na_{12}[Zn_5W_{19}O_{68}]\cdot 46H_2O$ (Na–Zn_5WO), $K_{11}[Zn_2Mn^{III}_3W_{19}O_{69}]\cdot 27H_2O$ (K–$Zn_2Mn^{III}_3$WO), and $K_{11}[Zn_2Fe^{III}_3W_{19}O_{69}]\cdot 44H_2O$ (K–$Zn_2Fe^{III}_3$WO) intercalated LDHs, which catalyzed the oximation of aromatic aldehydes with aqueous H_2O_2 as the oxidant in the absence of organic solvents. The Zn_3Al–$Zn_2Mn^{III}_3$WO heterogeneous catalyst exhibited a much higher selectivity (85%) than the homogeneous counterpart (55%). It was proposed that the synergistic interaction between the LDH host and intercalated POM anions plays a key role in the high oxime selectivity.

Other types of well-known homogeneous catalysts have also been immobilized in LDH hosts. For example, Wei *et al.*[89,90] reported a heterogeneous catalyst in which the rhodium complex (*trans*-RhCl(CO)(TPPTS-Na_3)$_2$) (TPPTS = tris(3-sulfophenyl)-phosphine trisodium salt) was intercalated in Zn/Al-LDHs, affording improved selectivity (up to 80%) in the hydroformylation of higher olefins. The authors proposed that the ordered arrangement of the intercalated rhodium complex anions played a key role in improving the selectivity, activity and stability. The strong electrostatic interactions between the LDH layers and the active rhodium species inhibited leaching of the active species and led to good catalyst reusability.

More recently, the investigation of heterogeneous chiral metal complex catalysts has attracted much interest, especially in the case of LDH-intercalated materials. In addition to increasing the yield of the reaction, in many cases intercalation of a chiral catalyst in an LDH host has been shown to afford

View Article Online

Published on 03 May 2013. Downloaded on 07/06/2013 03:35:59.

increases in enantioselectivity. This has been attributed to the controlled orientation and/or degree of dispersion of the intercalated active species. For example, Bhattacharjee and Anderson *et al.*[91,92] prepared chiral salen-Mn(III) complex intercalated Zn/Al-LDH catalysts. The resulting catalysts were found to be highly active and enantioselective in the epoxidation of various styrenes and cyclic alkenes when using a combination of pivalaldehyde and molecular oxygen at atmospheric pressure and room temperature. With 94% conversion, 1-methyl-1-cyclohexene could be converted to the epoxide with 68% ee and 90% selectivity with a TOF of 234 h^{-1}, whereas 4-methylstyrene was converted with 62% ee and 70% selectivity with a TOF of 327 h^{-1}.[92] In the case of styrenes and cyclic alkenes, TOF decreased as follows: α-methylstyrene > 4-methylstyrene > styrene and 1-methyl-1-cyclohexene > 1-phenyl-1-cyclohexene > cyclohexene. The catalyst could be recycled without detectable loss of efficiency. He's group[93,94] reported the intercalation of chiral Sharpless titanium tartrate catalysts in Mg/Al-LDH hosts. Dark-field TEM confirmed the highly-dispersed distribution of Ti active sites. Through tailoring the charge density of the brucite-like layers, the density of the interlayer titanium tartrate anions could be reliably tuned, giving an interdigitated bilayer arrangement. When used as a catalyst for the heterogeneous sulfoxidation of the prochiral methyl phenyl sulfide, the ee value was boosted from the negligible value observed for the homogeneous counterpart to 50%.[93] The two-dimensional interlayer space can be swollen by addition of various organic solvents (*e.g.*, CH_3CN or $MeOH/CH_2Cl_2$) during the reaction process, and thus accommodates the reactants in the interlayer. However it was found that the ee value decreased when the interlayer spacing was increased by a large swelling of the interlayer spacing. This confirms the role of the confinement effect of the LDH layers in enhancing the catalytic properties of an intercalated species.[94] He's group[95] further developed heterogeneous titanium tartrate intercalated LDHs by *in situ* coordination of the pre-intercalated L-tartrate anions as chiral ligands to the Ti(IV) center within the LDH galleries. The tartrate ligands were tuned to adopt a perpendicular- or horizontal-orientation to further control the coordination mode to the Ti(IV) center. It was found that the catalytic sites with the tartrate ligand in the perpendicular-standing orientation with the Ti(IV) center coordinated in both C–O–Ti and C=O–Ti modes displayed higher catalytic activity (93%) and better chiral induction (58%) in the asymmetric sulfoxidation than the corresponding horizontal-orientation. A catalytic mechanism was also proposed, as illustrated in Fig. 7.

As an extension of this idea, He *et al.*[38,96] showed vanadium(V) and zinc(II) centers could also be coordinated to pre-intercalated α-amino anions, showing significantly enhanced enantioselectivity in the asymmetric epoxidation, as also noted above in Section 2. The crucial role of the inorganic nanosheets as planar substituents in improving the enantioselectivity of the reaction was subsequently revealed by correlating the observed enantiomeric excess with the distribution of the catalytic centers and the accessibility of the substrate molecules to the catalytic sites. Density functional theory (DFT) calculations indicated that the LDH layer improves the enantioselectivity by influencing the formation and stability of the catalytic transition states, both in terms of steric hindrance and hydrogen bonding interactions.[39,40]

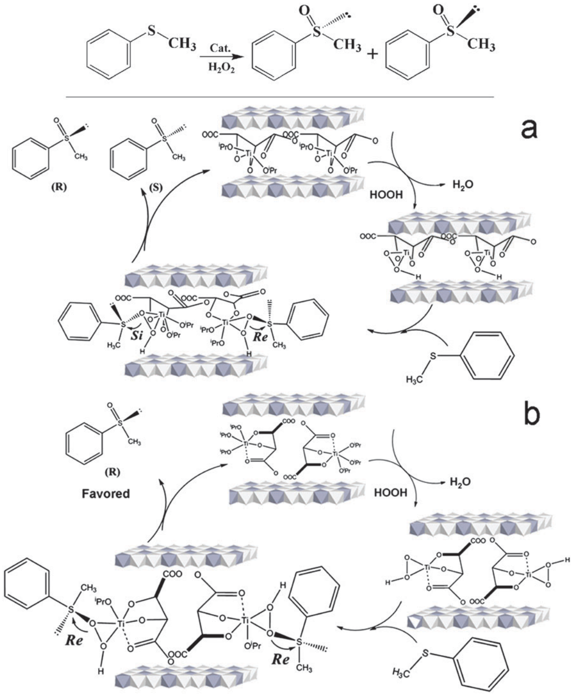

Fig. 7 The heterogeneous catalytic mechanism for the asymmetric sulfoxidation by a Ti(IV) tartrate complex intercalated in an LDH host with the tartrate ligands in (a) horizontal- or (b) perpendicular-orientation in the pre-intercalation process. Reproduced with permission from ref. 95.

LDHs are recognized to be more biocompatible and less toxic than most other inorganic nanoparticles, which allows even biocatalysts to be intercalated in LDH hosts.[97] The immobilization of enzymes in the interlayer region of LDHs has been shown to lead to significantly enhanced catalytic efficiency. For example, porcine pancreatic lipase (PPL) intercalated LDHs have been fabricated by an electrostatic-induced interfacial assembly, which could be tailored to control the PPL orientation, with the majority of active sites facing the LDH layer or facing adjacent protein molecules.[98] The activity of the intercalated PPL in the former orientation in the hydrolysis of glyceryl triacetate reached 445% (relative to the pristine enzyme). In addition, the thermal stability of PPL was significantly improved after intercalation. The apparent unfolding transition midpoint increased from *ca.* 323 K for pristine PPL to 364 K for intercalated PPL, when the majority of active sites were orientated facing the LDH layer. In the case of hemoglobin (Hb),[99] the intercalated Hb possesses only one orientation, but also exhibits significantly enhanced bioactivity and stability over pristine Hb in the oxidation of *o*-phenylenediamine (OPD) to phenazine.

5. Conclusion

This *Feature Article* summarizes the recent progress in the design and the preparation of nanocatalysts with high efficiency based on LDHs, including—but not limited to—exfoliation of the brucite-like layers, lattice orientation/lattice confinement by

Published on 03 May 2013. Downloaded on 07/06/2013 03:35:59.

the brucite-like layers, and the intercalation of active species. By virtue of the versatile chemical composition of LDH materials, nanocatalysts with preferential orientation, high dispersion and good stability can be fabricated, exhibiting excellent catalytic performance and recyclability. However, there are still great challenges in the design and the application of nanostructured catalysts based on LDH precursors: (i) generally speaking, the LDH nanosheets can only be stabilized in a small number of solvents, which restricts the range of catalyst species which can be assembled with the LDH nanosheets; (ii) during the topotactic transformation of LDH precursors into MMO materials, the lattice orientation/lattice confinement effect has not been well understood to date and more detailed and thorough investigation is needed; (iii) the mechanism of catalysis by intercalated active species confined in the 2D galleries of LDHs as well as the host–guest synergistic effects deserve deeper study. By overcoming the above challenges, the design and controlled synthesis of enhanced LDH-based materials should make a great contribution to the development of new practical catalysts.

Acknowledgements

We would like to thank all the co-workers cited in the references below for their invaluable contributions to the work described here. We also acknowledge generous financial support from the National Natural Science Foundation of China, the 973 Project (2011CBA00504), the 863 Program (2010AA03A403), the Program for Changjiang Scholars and Innovative Research Teams in Universities (IRT1205), the Fundamental Research Funds for the Central Universities (ZY1214) and the Research Fund for the Doctoral Program of Higher Education of China (20120010120008).

Notes and references

1 J. D. Aiken and R. G. Finke, *J. Mol. Catal. A: Chem.*, 1999, **145**, 1.
2 R. Schlögl and S. B. Abd Hamid, *Angew. Chem., Int. Ed.*, 2004, **43**, 1628.
3 M. Che and C. O. Bennett, *Adv. Catal.*, 1989, **36**, 55.
4 G. C. Bond and D. T. Thompson, *Catal. Rev. Sci. Eng.*, 1999, **41**, 319.
5 M. Valden, X. Lai and D. W. Goodman, *Science*, 1998, **281**, 1647.
6 J. K. Nørskov, T. Bligaard, J. Rossmeisl and C. H. Christensen, *Nat. Chem.*, 2009, **1**, 37.
7 F. Studt, F. Abild-Pedersen, T. Bligaard, R. Z. Sørensen, C. H. Christensen and J. K. Nørskov, *Science*, 2008, **320**, 1320.
8 F. Besenbacher, I. Chorkendorff, B. S. Clausen, B. Hammer, A. M. Molenbroek, J. K. Nørskov and I. Stensgaard, *Science*, 1998, **279**, 1913.
9 K. B. Zhou and Y. D. Li, *Angew. Chem., Int. Ed.*, 2012, **51**, 602.
10 F. Zaera, *Chem. Soc. Rev.*, 2013, **42**, 2746.
11 X. Y. Liu, M. H. Liu, Y. H. Luo, C. Y. Mou, S. D. Lin, H. K. Cheng, J. M. Chen, J. F. Lee and T. S. Lin, *J. Am. Chem. Soc.*, 2012, **134**, 10251.
12 X. W. Liu, K. B. Zhou, L. Wang, B. Y. Wang and Y. D. Li, *J. Am. Chem. Soc.*, 2009, **131**, 3140.
13 S. H. Joo, J. Y. Park, J. R. Renzas, D. R. Butcher, W. Y. Huang and G. A. Somorjai, *Nano Lett.*, 2010, **10**, 2709.
14 H. J. Zhang, T. Watanabe, M. Okumura, M. Haruta and N. Toshima, *Nat. Mater.*, 2012, **11**, 49.
15 B. T. Qiao, A. Q. Wang, X. F. Yang, L. F. Allard, Z. Jiang, Y. T. Cui, J. Y. Liu, J. Li and T. Zhang, *Nat. Chem.*, 2011, **3**, 634.
16 M. W. Small, S. I. Sanchez, L. D. Menard, J. H. Kang, A. I. Frenkel and R. G. Nuzzo, *J. Am. Chem. Soc.*, 2011, **133**, 3582.
17 R. T. Mu, Q. Fu, H. Xu, H. Zhang, Y. Y. Huang, Z. Jiang, S. Zhang, D. L. Tan and X. H. Bao, *J. Am. Chem. Soc.*, 2011, **133**, 1978.
18 J. A. Gursky, S. D. Blough, C. Luna, C. Gomez, A. N. Luevano and E. A. Gardner, *J. Am. Chem. Soc.*, 2006, **128**, 8376.
19 G. R. Williams and D. O'Hare, *J. Mater. Chem.*, 2006, **16**, 3065.
20 L. Desigaux, M. B. Belkacem, P. Richard, J. Cellier, P. Léone, L. Cario, F. Leroux, C. Taviot-Guého and B. Pitard, *Nano Lett.*, 2006, **6**, 199.
21 M. Fogg, A. L. Rohl, G. M. Parkinson and D. O'Hare, *Chem. Mater.*, 1999, **11**, 1194.
22 K. H. Goh, T. T. Lim and Z. L. Dong, *Water Res.*, 2008, **42**, 1343.
23 H. C. Liu and E. Z. Min, *Green Chem.*, 2006, **8**, 657.
24 F. Figueras, M. L. Kantam and B. M. Choudary, *Curr. Org. Chem.*, 2006, **10**, 1627.
25 J. T. Feng, Y. J. Lin, D. G. Evans, X. Duan and D. Q. Li, *J. Catal.*, 2009, **266**, 351.
26 X. Xiang, L. Bai and F. Li, *AIChE J.*, 2010, **56**, 2934.
27 S. Abelló, D. Verboekend, B. Bridier and J. Pérez-Ramírez, *J. Catal.*, 2008, **259**, 85.
28 L. He, Y. Q. Huang, A. Q. Wang, Y. Liu, X. Y. Liu, X. W. Chen, J. J. Delgado, X. D. Wang and T. Zhang, *J. Catal.*, 2013, **298**, 1.
29 P. J. Sideris, U. G. Nielsen, Z. H. Gan and C. P. Grey, *Science*, 2008, **321**, 113.
30 P. Liu, H. Wang, Z. C. Feng, P. L. Ying and C. Li, *J. Catal.*, 2008, **256**, 345.
31 Z. P. Liu, R. Z. Ma, M. Osada, N. Iyi, Y. Ebina, K. Takada and T. Sasaki, *J. Am. Chem. Soc.*, 2006, **128**, 4872.
32 C. X. Qi, J. C. Amphlett and B. A. Peppley, *Appl. Catal., A*, 2006, **302**, 237.
33 H. Morioka, Y. Shimizu, M. Sukenobu, K. Ito, E. Tanabe, T. Shishido and K. Takehira, *Appl. Catal., A*, 2001, **215**, 11.
34 F. Li, J. J. Liu, D. G. Evans and X. Duan, *Chem. Mater.*, 2004, **16**, 1597.
35 Q. Wang and D. O'Hare, *Chem. Rev.*, 2012, **112**, 4124.
36 F. Wypych, A. Bail, M. Halma and S. Nakagaki, *J. Catal.*, 2005, **234**, 431.
37 S. Liu, X. Jiang and G. Zhuo, *J. Mol. Catal. A: Chem.*, 2008, **290**, 72.
38 J. Wang, L. Zhao, H. Shi and J. He, *Angew. Chem., Int. Ed.*, 2011, **50**, 9171.
39 L. W. Zhao, H. M. Shi, J. Z. Wang and J. He, *Chem.–Eur. J.*, 2012, **18**, 9911.
40 L. W. Zhao, H. M. Shi, J. Z. Wang and J. He, *Chem.–Eur. J.*, 2012, **18**, 15323.
41 J. L. Gunjakar, T. W. Kim, H. N. Kim, I. Y. Kim and S. J. Hwang, *J. Am. Chem. Soc.*, 2011, **133**, 14998.
42 M. F. Shao, J. B. Han, W. Y. Shi, M. Wei and X. Duan, *Electrochem. Commun.*, 2010, **12**, 1077.
43 J. B. Han, X. Y. Xu, X. Y. Rao, M. Wei, D. G. Evans and X. Duan, *J. Mater. Chem.*, 2011, **21**, 2126.
44 J. W. Zhao, X. G. Kong, W. Y. Shi, M. F. Shao, J. B. Han, M. Wei, D. G. Evans and X. Duan, *J. Mater. Chem.*, 2011, **21**, 13926.
45 C. Li, L. Y. Wang, M. Wei, D. G. Evans and X. Duan, *J. Mater. Chem.*, 2008, **18**, 2666.
46 X. F. Zhao, F. Z Zhang, S. L. Xu, D. G. Evans and X. Duan, *Chem. Mater.*, 2010, **22**, 3933.
47 M. Zhao, Q. Zhang, W. Zhang, J. Huang, Y. Zhang, D. S. Su and F. Wei, *J. Am. Chem. Soc.*, 2010, **132**, 14739.
48 M. Q. Zhao, Q. Zhang, J. Q. Huang and F. Wei, *Adv. Funct. Mater.*, 2012, **22**, 675.
49 X. Xiang, H. Hima, H. Wang and F. Li, *Chem. Mater.*, 2008, **20**, 1173.
50 J. T. Feng, X. Y. Ma, Y. F. He, D. G. Evans and D. Q. Li, *Appl. Catal., A*, 2012, **413–414**, 10.
51 Y. Wang, J. Wang, G. Fan and F. Li, *Catal. Commun.*, 2012, **19**, 56.
52 L. He, Y. Q. Huang, A. Q. Wang, X. D. Wang, X. W. Chen, J. J. Delgado and T. Zhang, *Angew. Chem., Int. Ed.*, 2012, **51**, 6191.
53 M. Koike, D. L. Li, Y. Nakagawa and K. Tomishige, *ChemSusChem*, 2012, **5**, 2312.
54 Ota, E. L. Kunkes, I. Kasatkin, E. Groppo, D. Ferri, B. Poceiro, R. M. N. Yerga and M. Behrens, *J. Catal.*, 2012, **293**, 27.
55 S. He, S. T. Zhang, J. Lu, Y. F. Zhao, J. Ma, M. Wei, D. G. Evans and X. Duan, *Chem. Commun.*, 2011, **47**, 10797.
56 J. T. Feng, X. Y. Ma, Y. F. He, D. G. Evans and D. Q. Li, *Appl. Catal., A*, 2012, **413–414**, 10.
57 X. Y. Ma, Y. Y. Chai, D. G. Evans, D. Q. Li and J. T. Feng, *J. Phys. Chem. C*, 2011, **115**, 8693.
58 B. M. Choudary, S. Madhi, N. S. Chowdari, M. L. Kantam and B. Sreedhar, *J. Am. Chem. Soc.*, 2002, **124**, 14127.

Published on 03 May 2013. Downloaded on 07/06/2013 03:35:59.

59 F. Z. Zhang, X. F. Zhao, C. H. Feng, B. Li, T. Chen, W. Lu, X. D. Lei and S. L. Xu, *ACS Catal.*, 2011, **1**, 232.

60 S. Cho, J. W. Jang, S. Hwang, J. S. Lee and S. Kim, *Langmuir*, 2012, **28**, 17530.

61 P. Liu, Y. J. Guan, R. A. V. Santen, C. Li and E. J. M. Hensen, *Chem. Commun.*, 2011, **47**, 11540.

62 Mori, H. Abet and S. Inoue, *Appl. Organomet. Chem.*, 1995, **9**, 189.

63 N. T. Whilton, P. J. Vickers and S. Mann, *J. Mater. Chem.*, 1997, **7**, 1623.

64 S. Aisawa, S. Takahashi, W. Ogasawara, Y. Umetsu and E. Narita, *J. Solid State Chem.*, 2001, **162**, 52.

65 S. Aisawa, H. Kudo, T. Hoshi, S. Takahashi, H. Hirahara, Y. Umetsu and E. Narita, *J. Solid State Chem.*, 2004, **177**, 3987.

66 H. Nakayama, N. Wada and M. Tsuhako, *Int. J. Pharm.*, 2004, **269**, 469.

67 S. Aisawa, S. Sasaki, S. Takahashi, H. Hirahara, H. Nakayama and E. Narita, *J. Phys. Chem. Solids*, 2006, **67**, 920.

68 M. X. Reinholdt and R. J. Kirkpatrick, *Chem. Mater.*, 2006, **18**, 2567.

69 S. Li, *Colloids Surf., A*, 2006, **290**, 56.

70 Q. Yuan, M. Wei, D. G. Evans and X. Duan, *J. Phys. Chem. B*, 2004, **108**, 12381.

71 M. Wei, Q. Yuan, D. G. Evans, Z. Wang and X. Duan, *J. Mater. Chem.*, 2005, **15**, 1197.

72 M. Wei, X. Y. Xu, J. He, Q. Yuan, G. Y. Rao, D. G. Evans, M. Pu and L. Yang, *J. Phys. Chem. Solids*, 2006, **67**, 1469.

73 Z. An, W. Zhang, H. Shi and J. He, *J. Catal.*, 2006, **241**, 319.

74 S. Vijaikumar, A. Dhakshinamoorthy and K. Pitchumani, *Appl. Catal., A*, 2008, **340**, 25.

75 F. V. Laar, D. D. Vos, D. Vanoppen, B. Sels, P. A. Jacobs, G. A. Del, F. Pierard and M. A. Kirsch, *Chem. Commun.*, 1998, 267.

76 B. F. Sels, D. E. De Vos and P. A. Jacobs, *J. Am. Chem. Soc.*, 2007, **129**, 6916.

77 C. A. S. Barbosa, A. M. D. C. Ferreira and V. R. L. Constantino, *J. Inorg. Chem.*, 2005, **8**, 1577.

78 K. Lang, P. Bezdička, J. L. Bourdelande, J. Hernando, I. Jirka, E. Káfuňková, F. Kovanda, P. Kubát, J. Mosinger and D. M. Wagnerová, *Chem. Mater.*, 2007, **19**, 3822.

79 B. M. Choudary, B. Bharathi, R. C. Venkat, K. M. Lakshmi and K. V. Raghavan, *Chem. Commun.*, 2001, 1736.

80 S. Bhattacharhee, T. J. Dines and J. A. Anderson, *J. Phys. Chem. C*, 2008, **112**, 14124.

81 Z. Tong, T. Shichi and K. Takagi, *Mater. Lett.*, 2003, **57**, 2258.

82 K. A. D. F. Castro, A. Bail, P. B. Groszewicz, G. S. Machado, W. H. Schreiner, F. Wypych and S. Nakagaki, *Appl. Catal., A*, 2010, **386**, 51.

83 P. Liu and C. Li, *J. Catal.*, 2009, **262**, 159.

84 P. Liu, H. Wang, Z. C. Feng, P. L. Ying and C. Li, *J. Catal.*, 2008, **256**, 345.

85 K. M. Parida, M. Sahoo and S. Singha, *J. Catal.*, 2010, **276**, 161.

86 T. C. O. M. Leod, M. N. Kopylovicha, M. F. C. G. Silva, K. T. Mahmudova and A. J. L. Pombeiro, *Appl. Catal., A*, 2012, **439–440**, 15.

87 L. Cota, E. Ramíreza, F. Medina, J. E. Sueiras, G. Layrac and D. Tichit, *Appl. Catal., A*, 2010, **382**, 272.

88 S. Zhao, J. Xu, M. Wei and Y. F. Song, *Green Chem.*, 2011, **13**, 384.

89 M. Wei, X. Zhang, D. G. Evans, X. Duan, X. Li and H. Chen, *AIChE J.*, 2007, **53**, 2916.

90 X. Zhang, M. Wei, M. Pu, X. Li, H. Chen, D. G. Evans and X. Duan, *J. Solid State Chem.*, 2005, **178**, 2701.

91 S. Bhattacharjee and J. A. Anderson, *Chem. Commun.*, 2004, 554.

92 S. Bhattacharjee and J. A. Anderson, *Adv. Synth. Catal.*, 2006, **348**, 151.

93 H. Shi, C. Yu and J. He, *J. Phys. Chem. C*, 2010, **114**, 17819.

94 H. Shi, C. Yu and J. He, *J. Catal.*, 2010, **271**, 79.

95 H. Shi and J. He, *J. Catal.*, 2011, **279**, 155.

96 H. Liu, L. Zhao, J. Wang and J. He, *J. Catal.*, 2013, **298**, 70.

97 S. J. Choi, J. M. Oh and J. H. Choy, *J. Mater. Chem.*, 2008, **18**, 615.

98 Z. An, J. He, S. Lu and L. Yang, *AIChE J.*, 2010, **56**, 2677.

99 Z. An, S. Lu, J. He and Y. Wang, *Langmuir*, 2009, **25**, 10704.

This journal is © The Royal Society of Chemistry 2013